

Transport study of a single bismuth nanowire fabricated by the silver and silicon nanowire shadow masks

D. S. Choi^{a)}

Electrical Engineering Department, University of California at Los Angeles, Los Angeles, California 90095

A. A. Balandin

Nano-Device Laboratory, Department of Electrical Engineering, University of California at Riverside, Riverside, California 92521

M. S. Leung, G. W. Stupian, and N. Presser

Electronics Photonics Laboratory, The Aerospace Corporation, El Segundo, California 90245

S. W. Chung^{b)} and J. R. Heath^{c)}

Department of Chemistry and Biochemistry, University of California, Los Angeles, California 90095

A. Khitun and K. L. Wang

Electrical Engineering Department, University of California at Los Angeles, Los Angeles, California 90095-1594

(Received 13 June 2006; accepted 8 August 2006; published online 6 October 2006)

The authors have carried out measurements of the electrical conductivity of single bismuth nanowires fabricated by the low energy electron beam lithography using the silver/silicon nanowire shadow masks. The examined nanowires had cross-sectional dimensions of 40×30 and 40×50 nm². The chosen nanowire sizes had been slightly below the critical diameter D (~ 50 nm) at which a semimetal to semiconductor phase transition was predicted to occur. The results reveal a semiconductorlike temperature dependence of the electrical conductivity of a bismuth nanowire, which is strikingly different from that of the bulk bismuth. © 2006 American Institute of Physics. [DOI: 10.1063/1.2357847]

Low-dimensional structures continue to attract considerable interest because of their great promise for applications in future electronic, optoelectronic, and thermoelectric devices.^{1,2} The potential advantage of these structures arises from spatial confinement of carriers and phonons and corresponding modification of their densities of states. Most recently the attention was focused on bismuth (Bi) quantum wires. While Bi is a semimetal in its bulk form, it was theoretically predicted that at the critical wire width of $D_g \sim 52$ nm a transition to the semiconductor phase occurs.³ Numerous high-speed electronic and thermoelectric applications have been suggested for Bi nanowires owing to their useful properties such as small effective mass, low thermal conductivity, long mean free path of the carriers, and the possibility of inducing the phase transition by quantum confinement.³

Despite predicted superior properties of Bi quantum wires, the experimental work has been far short of those done on other low-dimensional structures. This is primarily due to difficulties in fabrication of high quality crystalline Bi nanowires and in making good ohmic contacts to a single wire. To date the best experimental results achieved in this area was an investigation of magnetotransport of the *arrays* of Bi nanowires embedded in a porous alumina matrix.^{4,5} Recently, size-dependent transport and thermoelectric properties of polycrystalline Bi nanowires were studied

elsewhere.⁶ However, the measurements were done on about ten Bi nanowires and not a single nanowire and the examined nanowires were polycrystalline.⁶ In this letter, we report results of the transport study of a *single* and *crystalline* Bi quantum wire with the characteristic dimensions below the critical width D_o .

For this study, Bi nanowires with widths of 50 and 30 nm were fabricated by low energy electron beam lithography using organically functionalized silver (Ag) nanocrystal nanowires and silicon (Si) nanowires as shadow masks. Figure 1 shows field emission scanning electron microscope (FESEM) images of the 50 and 30 nm wide Bi nanowires to which platinum (Pt) submicron-size contacts have been made by *in situ* focused ion beam (FIB) metal deposition. The 40 nm thick Bi single-crystal films were grown on indium doped semi-insulating CdTe (111)*B* substrates by molecular beam epitaxy (MBE). The crystal quality and orientation of MBE-grown Bi films with rhombohedral crystal structure were investigated by x-ray diffraction (XRD) experiments. The XRD powder patterns shown in Fig. 2 revealed only sharp (000*l*) peaks, which implied *c*-axis growth of Bi perpendicular to the substrates.

The low energy electron beam lithography using the Ag nanocrystal shadow mask process was reported earlier.⁷ The self-assembled high-aspect-ratio Ag nanocrystal wires were prepared by organically functionalized Ag nanoparticles 3 nm in diameter. The wires were found to keep their structures aligned with an interwire separation of just a few nanometers.⁸ The nanocrystal Langmuir film was then transferred as a Langmuir-Schaeffer film to 40 nm thick polymethyl methacrylate (PMMA) coated Bi/CdTe substrates. A FESEM was used to expose the samples to a 600 pA, 700 V

^{a)}Present address: Jet Propulsion Laboratory, California Institute of Technology, Pasadena, CA 91109; electronic mail: daniel.s.choi@jpl.nasa.gov

^{b)}Present address: Lawrence Livermore National Laboratory, Livermore, CA 94551.

^{c)}Present address: Department of Chemistry and Chemical Engineering, California Institute of Technology, Pasadena, CA 91109.

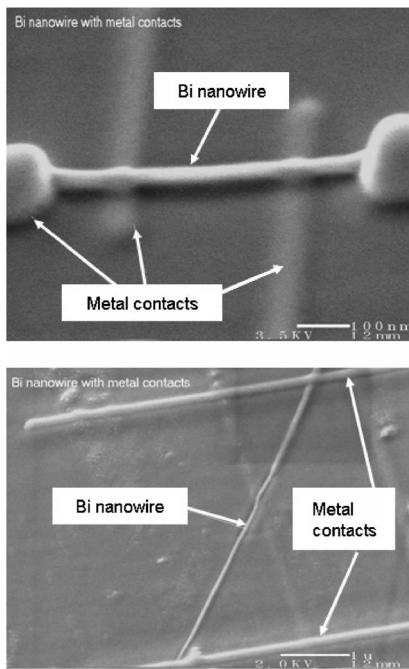


FIG. 1. FESEM micrographs of 50 nm wide (top) and 30 nm wide (bottom) Bi nanowires with metal contacts. *In situ* metal (Pt) contacts were prepared by FIB metal deposition.

electron beam over an area of $100 \times 100 \mu\text{m}^2$ for 10 min. The total electron dose to the PMMA was $50 \mu\text{C}/\text{cm}^2$. At 700 V, the electron stopping effective range for Ag was estimated to be about 4 nm, which is smaller than the thickness of the Ag nanocrystal shadow mask. Following the e-beam exposure, samples were developed for 1 min in a mixture of methyl isobutyl ketone and isopropanol in the ratio of 3:1. As a result of a subsequent reactive ion etching process using a mixture of BCl_3 and Ar_2 gases, 50 nm wide and 40 nm high Bi nanowires were fabricated on the indium doped semi-insulating CdTe substrates.

Similarly, 30 nm wide, 40 nm high Bi nanowires were fabricated using the same technique with a Si nanowire shadow mask. Si nanowires were prepared by a vapor-liquid-solid process.⁹

The measured temperature dependence of the electrical conductivity (σ) of a single Bi nanowire is shown in Fig. 3. A four-point probe geometry was employed to avoid effects from contact resistances for temperature-dependent I - V measurements on a single Bi nanowire. On both the 30 and 50 nm wires, the conductivity increases with increasing tem-

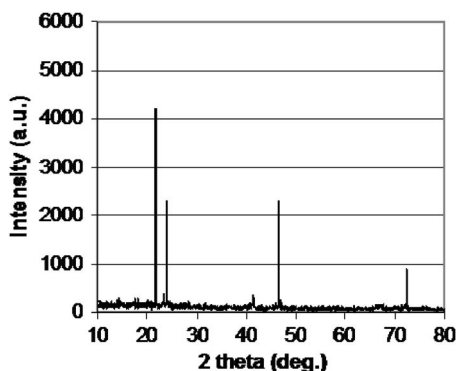


FIG. 2. X-ray diffraction pattern of MBE-grown Bi film on CdTe (111)B substrate.

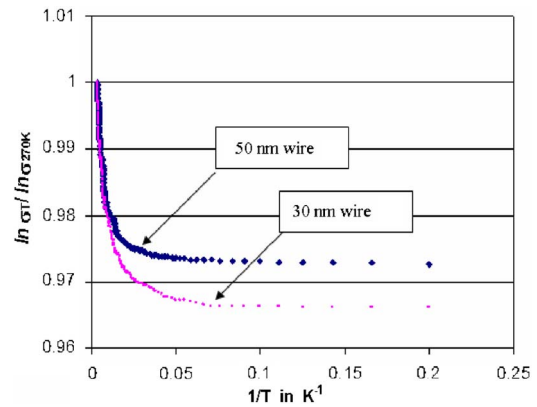


FIG. 3. Normalized temperature dependence of the conductivity of a single Bi nanowire with widths of 50 and 30 nm.

perature. This temperature dependence is characteristic of semiconductors and not semimetals. It is known that the conductivity of metals and semiconductors approximately obeys the relationship $\sigma = \sigma_0 / (1 + \alpha T)$, where α is the temperature coefficient, T is the temperature in $^\circ\text{C}$, and σ_0 is the conductivity at 0°C . For metals $\alpha > 0$, while for intrinsic semiconductors $\alpha < 0$. For bulk Bi, $\alpha = 4.2 \times 10^{-4} \text{K}^{-1}$ in the temperature range $t = 0 - 100^\circ\text{C}$. Thus, in the case of our narrow quantum wires the measured results indeed show that the Bi nanowire is in its semiconductor rather than the semimetal form. This experimental observation is in line with theoretical predictions of the critical wire width of $D = 52 \text{ nm}$ at which the semiconductor-semimetal transition occurs.³

The quantitative description of the electrical conductivity requires the knowledge of the thermal activation process for a particular material as well as the type of doping. The intrinsic carrier density increases exponentially with the temperature as

$$\sigma = \sigma_0 \exp\left(-\frac{E_g}{2kT}\right), \quad (1)$$

where σ_0 is a preexponential constant, E_g the energy band gap, k the Boltzmann constant, and T the absolute temperature.

One may also notice in Fig. 3 that the conductivity of a 30 nm wide Bi nanowire becomes much smaller than that of a 50 nm wide Bi nanowire as temperature decreases. In order to explain this we use the formalism developed for a one-dimensional conductor:^{10,11}

$$\sigma = D_e \left[\frac{1}{2} F_{-1/2}^e \right] + D_h \left[\frac{1}{2} F_{-1/2}^h \right], \quad (2)$$

where D_e and D_h are given by

$$D_e = \frac{2e}{\pi a^2} \left(\frac{2k_B T}{h^2} \right)^{1/2} m_e^{1/2} \mu_{e,h},$$

$$D_h = \frac{2e}{\pi a^2} \left(\frac{2k_B T}{h^2} \right) m_h^{1/2} \mu_{e,h}. \quad (3)$$

Here F_i are the Fermi-Dirac functions of $\frac{1}{2}$ order, and m_e , m_h , μ_e , and μ_h are the effective masses and mobilities along the transport direction for electron and holes, respectively. The reduced chemical potentials for electron and holes are related to each other as

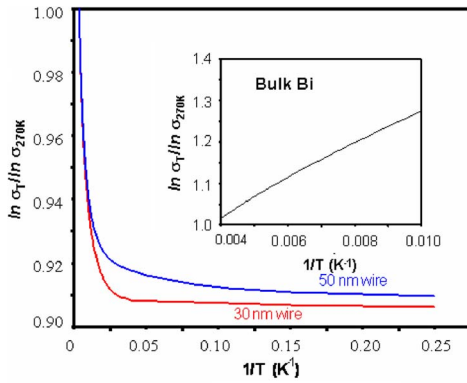


FIG. 4. Calculated normalized temperature dependence of the conductivity of a single Bi nanowire with widths of 50 and 30 nm.

$$\zeta_e^* + \zeta_h^* = -\Delta/k_B T, \quad (4)$$

where Δ is the energy gap in the presence of quantum confinement. The effect of quantum confinement leads to the energy gap dependence on the wire width as given by the equation

$$\Delta = \Delta_{\text{bulk}} + \frac{\hbar^2 \pi^2}{2m_y^{e,h} a^2} + \frac{\hbar^2 \pi^2}{2m_z^{e,h} a^2}. \quad (5)$$

As a result, energy gap increases with the decreasing wire width. A phase transition from the semimetal ($\Delta_{\text{bulk}} = -38$ meV) to semiconductor ($\Delta > 0$) is predicted by this formalism for Bi nanowire at some “critical” wire width $a = 52.1$ nm ($\Delta = 0$).³ The phase transition drastically changes the temperature dependence of the electrical conductivity.

Another important factor that affects the conductivity is the change in mobility as the wire width decreases. At low enough temperature, when the elastic scattering is dominant, mobility is predicted to increase in quantum wires due to the restriction of the phase space for scattering.¹² At moderate temperatures and for quantum wires with finite lateral dimensions the opposite trend can be observed. The mobility of a nanowire can also be affected by the change in the electron-phonon scattering rates due to the confinement-induced phonon spectrum modification in a nanowire.¹² In our calculations we used the following approximate expression for the mobility dependence on the nanowire radius $\mu = \mu(a)$ due to scattering on optical phonons:¹³

$$\frac{\mu_{1D}^{\text{op}}}{\mu_{3D}^{\text{op}}} = 8K_1(\hbar\omega_0/(2k_B T)) \left[3 \int_0^\infty dx E_1 \left(\frac{a^2 x}{8l^2} - \frac{\hbar\omega_0}{2k_B T x} - \frac{\hbar\omega_0 x}{8k_B T x} \right) \right]^{-1}, \quad (6)$$

where K_1 is the modified Bessel function of the second kind, $E_1(x)$ is the exponential integral function, $l^2 = \hbar/2\pi m_x \omega_0$, and ω_0 is the limiting phonon frequency.

Using Eqs. (1)–(6) we have calculated the electron mobility and electrical conductivity in Bi nanowires. We developed a model that describes the temperature dependence of the electrical conductivity of Bi quantum wires. Figure 4 shows the calculated dependence of $\ln \sigma$ vs T^{-1} for 50 and 30 nm Bi wires. The obtained results are in good agreement with experimental data (see Fig. 3). The E_g value extracted from the slope in Fig. 3 is about 10 meV. The conduction subband and valence subband edges move in opposite direc-

tions to eventually form a positive energy band gap E_g between the lowest L -point conduction subband edge and highest T -point valence band edge. Thus, our work provided for the first time a comparison between the calculated and experimental electron conductivities of a single Bi nanowire with the width smaller than the critical width. The model which we developed takes into account quantum confinement effects via the reduced chemical potential and modification of the mobility due to changed electron-phonon scattering in a quantum wire. The semiconductorlike behavior of the electrical conductivity of a single quantum wire was explained by the phase transition that occurred when the wire thickness dropped below $D_o \sim 52$ nm.

To summarize, we fabricated the 50 and 30 nm wide single Bi nanowires and measured the temperature dependence of their electrical conductivity. For a narrower wire, the electrical conductivity was found to be smaller because of the reduced mobility. The energy band gap of the semiconductorlike Bi nanowire has been estimated to be about 10 meV, which is in agreement with our calculations. The reported increase in electrical conductivity of Bi at higher temperatures is important for suggested thermoelectric applications of Bi wire arrays. The increase in the electrical conductivity σ_e combined with the decrease in the thermal conductivity κ of the quantum wires¹² may lead to higher values of the thermoelectric figure of merit $ZT = S^2 \sigma_e T / \kappa$ (where S is the thermoelectric power and κ is the thermal conductivity).

The authors gratefully acknowledge support for this work by Augmentation Awards for Science and Engineering Research Training (AASERT) Fellowship Grant No. N00014-96-1-1258, the Office of Naval Research (ONR) MURI, the ARO MURI, and the U.S. Air Force under Contract No. F04701-93-C-0094. One of the authors (J.R.H.) acknowledges ONR Contract No. N00014-981-0422. Two of the authors (K.L.W. and J.R.H.) also acknowledge the support of the Semiconductor Research Corporation. One of the authors (A.A.B.) acknowledges NSF and NASA support.

¹Y. Liu and R. E. Allen, Phys. Rev. B **52**, 1566 (1995).

²A. Svizhenko, A. Balandin, and S. Bandyopadhyay, J. Appl. Phys. **81**, 7927 (1997).

³X. Sun, Z. Zhang, and M. S. Dresselhaus, Appl. Phys. Lett. **74**, 4005 (1999).

⁴Z. Zhang, M. S. Dresselhaus, and X. Sun, Appl. Phys. Lett. **73**, 1589 (1998).

⁵K. Heremans, Phys. Rev. B **58**, R10091 (1998).

⁶A. Boukai, K. Xu, and J. Heath, Adv. Mater. (Weinheim, Ger.) **18**, 864 (2006).

⁷S. H. Choi, K. L. Wang, M. S. Leung, G. W. Stupian, N. Presser, S. W. Chung, G. Markovich, S. H. Kim, and J. R. Heath, J. Vac. Sci. Technol. A **17**, 1425 (1999).

⁸S. W. Chung, G. Markovich, and J. R. Heath, J. Phys. Chem. **102**, 6685 (1998).

⁹J. T. Hu, T. W. Odom, and C. M. Lieber, Acc. Chem. Res. **32**, 435 (1999).

¹⁰N. W. Ashcroft and N. D. Mermin, *Solid State Physics* (Holt, Rinehart and Winston, New York, 1976), Chap. 13, p. 126.

¹¹A. Casian, I. Sur, A. Sandu, H. Scherrer, and S. Scherrer, *ICT'97 Proceedings of the 16th International Conference on Thermoelectrics, Dresden, Germany, 1997* (IEEE, Piscataway, NJ, 1998), IEEE Catalog No. 97th 8291, p. 442; I. Sur, A. Casian, and A. A. Balandin, Phys. Rev. B **69**, 035306 (2004).

¹²H. Sakaki, Jpn. J. Appl. Phys., Part 2 **19**, L735 (1980).

¹³A. Balandin and K. L. Wang, J. Appl. Phys. **84**, 6149 (1998); Phys. Rev. B **58**, 1544 (1998); J. Zou and A. Balandin, J. Appl. Phys. **89**, 2932 (2001).